

Mechanical Collapse Testing on Aluminum Stiffened Plate Structures for Marine Applications

Jeom Kee Paik¹⁾, Celine Andrieu²⁾, and H. Paul Cojeen³⁾

¹⁾ Pusan National University, Korea, ²⁾ Alcan Marine, France, ³⁾ U.S. Coast Guard, USA

Abstract

The present paper is a summary of the R&D results obtained through SSC SR-1446 project sponsored by Ship Structure Committee together with Alcan Marine, France. It is recognized that the use of ultimate limit state (ULS) design method in addition to more conventional structural design standards will help make possible to move high speed vessels to open ocean transiting of very large high speed vessels, which is what the US Navy is certainly trying to do.

The aim of the project is to investigate the collapse characteristics of aluminum stiffened plate structures used for marine applications by mechanical testing, together with nonlinear FEA. Fabrication related initial imperfections significantly affect the ULS behavior, and thus it is of vital importance to identify the features of initial imperfections prior to ULS computations. In the present study, statistical database of fabrication related initial imperfections on welded aluminum stiffened plate structures is also developed. The database and insights developed will be very useful for design and building of welded aluminum high-speed ocean-going vessel structures.

Keywords

Aluminum stiffened plate structures; High-speed ocean-going vessels; Ultimate limit state design; Mechanical collapse testing; Fabrication related initial imperfections; Nonlinear finite element analysis.

Introduction

The use of high strength aluminum alloys in shipbuilding provides many benefits but also presents many challenges. The benefits of using aluminum versus steel include lighter weight, which helps increase cargo capacity and/or reduce power requirements, excellent corrosion resistance and low maintenance. Challenges include reduced stiffness causing greater sensitivity to deformation, buckling, and plastic collapse and different welding practices.

The benefits noted above are now well recognized, particularly for the design and construction of war ships, littoral surface crafts, and littoral combat ships as well

as fast passenger ships. The size of such ships is increasing, causing various related design challenges compared to vessels with shorter length. In addition to aluminum alloys being less stiff than mild steel, no refined ultimate limit state (ULS) design methods involving local and overall ULS assessment exist unlike steel structures where the necessary information is plentiful. The use of ULS design method in addition to more conventional structural design standards will be able to help design and build very large ocean-going aluminum high speed vessel structures.

The present paper is a summary of the R&D results obtained through SSC SR-1446 project sponsored by Ship Structure Committee together with Alcan Marine, France. Buckling collapse characteristics of welded aluminum stiffened plate structures were investigated by mechanical testing on a total of 78 single- and multi-bay prototype structures, which are full scale equivalent to subs-structures of an 80m long aluminum high speed vessel structure. Welding induced initial imperfections significantly affect the ULS behavior, and it is thus of vital importance to identify the features of initial imperfections prior to the ULS computations and design. In this regard, the statistics of welding induced initial imperfections on the prototype structures are measured and analyzed. The buckling collapse testing is undertaken until and after the ULS is reached. Nonlinear FEA solutions are also obtained for the prototype structures. Based on the experimental and numerical results, closed-form ULS formulae are developed.

In the past, useful studies on mechanical collapse testing of welded aluminum structures have of course been undertaken. In the early 1980s, a series of 76 aluminum un-stiffened plate collapse tests were carried out by Mofflin (1983) and Mofflin & Dwight (1984) at the University of Cambridge, UK; and these are regarded as perhaps one of the largest and most relevant test programs for the collapse strength of aluminum plating (un-stiffened plates) until now. After TIG (tungsten inert gas) welding in the longitudinal direction and MIG (metal inert gas) welding in the transverse direction, weld induced initial distortions and residual stresses were measured and their influences on the plate collapse behavior were studied on two of the most

common aluminum alloys used for the construction of high speed vessels, i.e., 5083 and 6082 alloys.

In the late 1980s, Clarke & Swan (1985) and Clarke (1987) at the Admiralty Research Establishment (ARE), UK carried out the buckling collapse testing on a total of five aluminum stiffened plate structures. This was one of the earliest collapse test programs to use ship-shaped aluminum stiffened plate structures using full-scale prototype models of all-welded construction with multiple frame bays. All material of the test structures was equivalent to 5083 aluminum alloy.

Over a decade after the ARE tests, several collapse test programs on aluminum stiffened plate structures constructed by welding were carried out together with various surveys of weld induced initial imperfections. These include Hopperstad et al. (1998, 1999), Tanaka & Matsuoka (1997), Matsuoka et al. (1999), Zha et al. (2000), Zha & Moan (2001, 2003) and Aalberg et al. (2001). The material of most test structures was 5083 aluminum alloy for plating and 6082 aluminum alloy for stiffeners.

Except perhaps for those by Tanaka & Matsuoka (1997) and Matsuoka et al. (1999) which were full-scale prototype models with multiple frame bays, most of these test structures were small scale models composed of a single stiffener with attached plating or a thin-walled cruciform structure. Although the nature and extent of test structures were somewhat limited, these test results were still very useful in studying the statistics of weld induced initial imperfections as well as the compressive collapse strength characteristics themselves.

Even in light of the existing excellent research results on the weld induced initial imperfections and ultimate strength of aluminum structures noted above, more studies are certainly required, because a systematic survey of the initial imperfection and buckling collapse characteristics is very lacking for a variety of aluminum alloy types and structural dimensions typical of ship-shaped full-scale prototype structures considering the recent trends in the application of aluminum marine structures.

A significant motive for initiating the present research project was to contribute to resolving the issue noted above to a good degree, by developing relevant design database on fabrication related initial imperfections and ultimate strength of welded aluminum stiffened plate structures for marine applications.

Design and fabrication of test structures

Table 1 indicates the overall dimensions of prototype structures. A total of 78 prototype aluminum structures that are full-scale equivalent to sub-structures of an 80m long all aluminum high-speed vessel are considered. They are designed in terms of single and multi-bay stiffened plate structures as those shown in Fig.1.

While various methods for fabricating aluminum ship structures are today relevant, the present test program adopts the MIG welding technique, which is

now one of the most popular methods of welding in aluminum ship construction.



Fig.1(a): One-bay prototype structure



Fig.1(b): Three-bay prototype structure

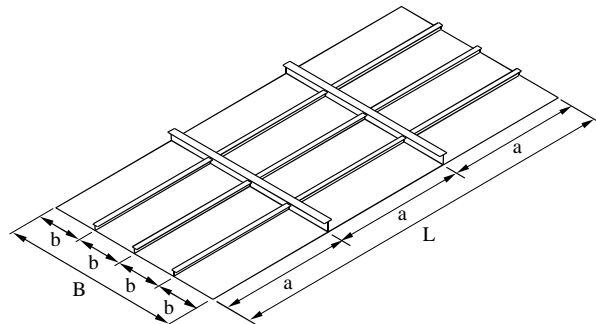


Fig.2: Nomenclature: A stiffened plate structure

To cover the possible diverse range of in-service aluminum marine structures representative of various collapse failure modes, a variety of structural dimensions, material types, plate thicknesses, stiffener types and stiffener web heights are considered as follows (see Fig.2 for the nomenclature):

- Panel width: $B = 1000$ mm;
- Stiffener spacing: $b = 300$ mm;
- Panel length: 1000 mm (one-bay structure), 1200 mm (one-bay structure), 3000 mm (three-bay structure of 1000 mm length);
- Material types: plate – 5083-H116 (rolled), 5383-H116 (rolled), stiffeners – 5083-H116 (rolled), 5383-H112 (extruded), 5383-H116 (rolled), 6082-T6 (extruded);

- Thickness: plate – 5 mm, 6 mm, 8 mm, stiffeners – 4 mm, 5 mm, 6 mm, 8 mm;
- Stiffener types: flat bar, built-up T-bar, extruded T-bar;
- Stiffener web height: 60 mm, 70 mm, 80 mm, 90 mm, 100 mm, 120 mm, 140 mm.

Table 2 indicates the minimum values of mechanical properties of aluminum alloys used for building the prototype structures.

Statistics of weld induced initial imperfections

When aluminum alloys are locally heated, the heated part will expand but because of adjacent cold part it will be subjected to compressive stress and distortion. When the heated part is cooled down, it will tend to locally shrink and thus now be subjected to a tensile stress. While the same happens in steel structures as well, it is the case that in aluminum structures the aluminum material in the HAZ is typically softened and subsequently the strength (yield stress) of the HAZ is generally reduced, which is termed a material softening phenomenon.

Figure 3 represents a profile of the weld induced initial distortions in a stiffened plate structure, where stiffeners distort in the direction of web and also sideways and plating deflects in the lateral direction. Due to welding, tensile residual stresses remain in the HAZ, and compressive residual stresses develop in the other areas to be in equilibrium of internal forces as shown in Fig.4. The distribution of residual stresses in plating which is welded along multiple stiffener lines or edges may differ from that in stiffener web itself as shown in Fig.5.

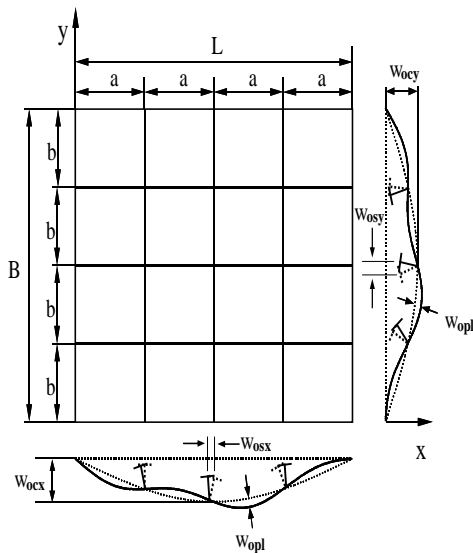


Fig.3: A profile of weld induced initial distortions in a stiffened plate structure

Figure 6 shows idealized schematics of softened regions in the HAZ. In the plating, since stiffeners are assumed to be welded in this case along all four edges, the softening zones develop along all edges as indicated. Its counterpart in the stiffener attached by welding is

also shown. In terms of structural behavior in association with softening in the HAZ, the breadth of the softening zones together with the reduction of yield strength plays a primary role in strength characterization.

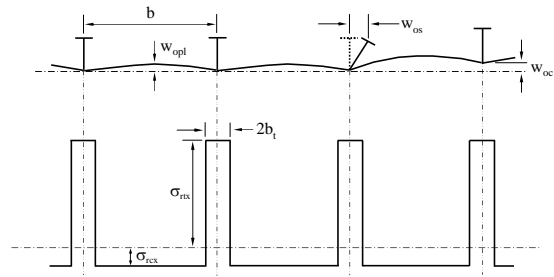


Fig.4: Weld induced initial distortions and residual stresses in a stiffened plate structure

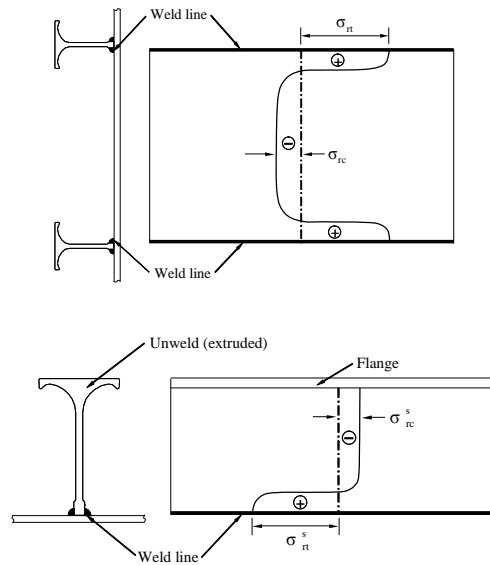


Fig.5: Schematics of the distribution of weld induced residual stresses in a plate welded at two edges, and in the stiffener web welded at one edge (left: plating, right: extruded stiffener web; +: tension, -: compression)

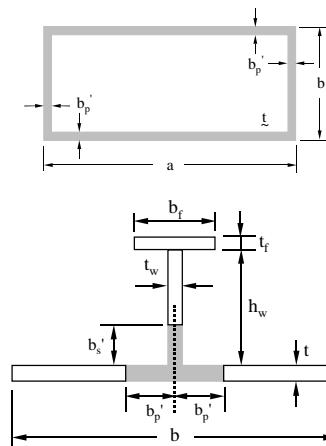


Fig.6: Idealized profiles of softened zones inside an aluminum plate welded at four edges, and its counterpart in the stiffener attachment to plating

While weld induced initial imperfections described above should be minimized by application of proper welding procedures and fabrication methods, it is nevertheless important to realize that their levels in specific cases can have a remarkable influence on the strength and stiffness of the structures. Hence their levels must be dealt with as parameters of influence in the analysis of load-carrying capacity. This means that such initial imperfection parameters must be properly determined in advance and accounted for in the design process including reliability analyses and code calibrations.

For aluminum stiffened plate structures constructed by welding, the following six types of initial imperfections will generally be pertinent, namely

- Initial distortion of plating between stiffeners;
- Column type initial distortion of stiffener;
- Sideways initial distortion of stiffener;
- Residual stresses of plating between stiffeners;
- Residual stresses of stiffener web;
- Softening in the HAZ in terms of reduction of the HAZ material yield stress and breadth of softened zone.

In the present study, the six types of initial imperfections noted above were measured for all the prototype structures (Paik et al. 2006, Paik 2007a). Figure 7 shows 3-dimensional configurations of selected test structures after welding, indicating initial distortions in terms of plate initial deflection, column type initial deflection of stiffeners, and sideways initial deflections of stiffeners. Figure 8 shows measurements of welding induced residual stresses in plating and stiffener web.

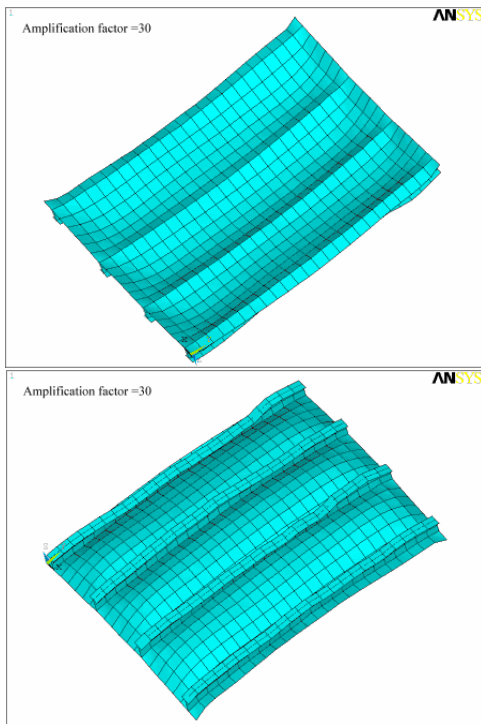


Fig.7(a): 3-dimensional displays of a selected prototype structure distorted after welding, for ID7 with amplification factor of 30

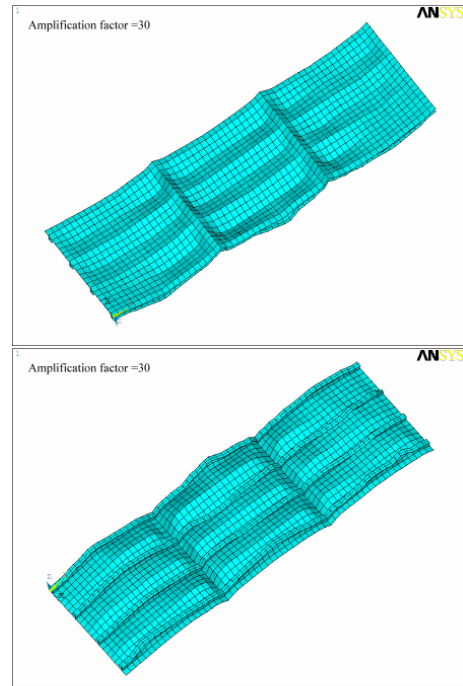


Fig.7(b): 3-dimensional displays of a selected prototype structure distorted after welding, for ID77 with amplification factor of 30

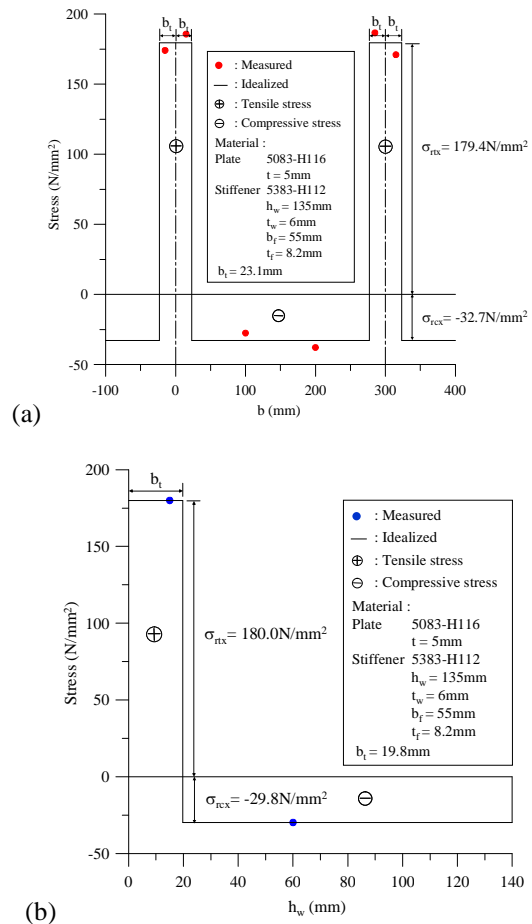


Fig.8: Residual stress distributions at (a) plating, (b) stiffener web for ID4 (5083-H116)

Based on the statistical analyses of the extensive initial imperfection measurements undertaken in the

present study, the levels of initial imperfection parameters useful for design as well as reliability analyses and code calibrations can be suggested when 5% and below band data is applied for the slight level analysis and 95% and above band data is applied for the severe level analysis, as follows

Maximum initial distortion of plating:

$$w_{opl} = \begin{cases} 0.018\beta^2 t & \text{for slight level} \\ 0.096\beta^2 t & \text{for average level} \\ 0.252\beta^2 t & \text{for severe level} \end{cases} \quad (1)$$

where $\beta = \frac{b}{t} \sqrt{\frac{\sigma_Y}{E}}$ = plate slenderness ratio.

One half-wave initial distortion amplitude of plating:

$$w_{ol} = \begin{cases} 0.0059\beta^2 t & \text{for slight level} \\ 0.093\beta^2 t & \text{for average level} \\ 0.252\beta^2 t & \text{for severe level} \end{cases} \quad (2)$$

Localized initial distortion of plating:

$$w_{ob} = \begin{cases} 0.00033\beta^2 t \approx 0.0 & \text{for slight level} \\ 0.010\beta^2 t & \text{for average level} \\ 0.0365\beta^2 t & \text{for severe level} \end{cases} \quad (3)$$

Buckling mode initial distortion of plating:

$$w_{om} = \begin{cases} 0.0 & \text{for slight level} \\ 0.00552\beta^2 t & \text{for average level} \\ 0.0468\beta^2 t & \text{for severe level} \end{cases} \quad (4)$$

Maximum column type initial distortion of stiffener:

$$w_{oc} = \begin{cases} 0.00016a & \text{for slight level} \\ 0.0018a & \text{for average level} \\ 0.0056a & \text{for severe level} \end{cases} \quad (5)$$

One half-wave column type initial distortion of stiffener:

$$w_{ol}^c = \begin{cases} 0.0 & \text{for slight level} \\ 0.00155a & \text{for average level} \\ 0.00525a & \text{for severe level} \end{cases} \quad (6)$$

Maximum sideways initial distortion of stiffener:

$$w_{os} = \begin{cases} 0.00019a & \text{for slight level} \\ 0.001a & \text{for average level} \\ 0.0024a & \text{for severe level} \end{cases} \quad (7)$$

One half-wave sideways initial distortion of stiffener:

$$w_{ol}^s = \begin{cases} 0.0 & \text{for slight level} \\ 0.000574a & \text{for average level} \\ 0.0018a & \text{for severe level} \end{cases} \quad (8)$$

Yield stress of the HAZ material for 5083-H116:

$$\frac{\sigma_{YHAZ}}{\sigma_Y} = \begin{cases} 0.906 & \text{for slight level} \\ 0.777 & \text{for average level} \\ 0.437 & \text{for severe level} \end{cases} \quad (9)$$

where $\sigma_Y = 215 \text{ N/mm}^2$.

Yield stress of the HAZ material for 5383-H116:

$$\frac{\sigma_{YHAZ}}{\sigma_Y} = \begin{cases} 0.820 & \text{for slight level} \\ 0.774 & \text{for average level} \\ 0.640 & \text{for severe level} \end{cases} \quad (10)$$

where $\sigma_Y = 220 \text{ N/mm}^2$.

Yield stress of the HAZ material for 5383-H112:

$$\frac{\sigma_{YHAZ}}{\sigma_Y} = 0.891 \text{ for average level} \quad (11)$$

where $\sigma_Y = 190 \text{ N/mm}^2$.

Yield stress of the HAZ material for 6082-T6:

$$\frac{\sigma_{YHAZ}}{\sigma_Y} = 0.703 \text{ for average level} \quad (12)$$

where $\sigma_Y = 240 \text{ N/mm}^2$.

Compressive residual stress at plating:

$$\sigma_{rcx} = \begin{cases} -0.110\sigma_{Yp} & \text{for slight level} \\ -0.161\sigma_{Yp} & \text{for average level} \\ -0.216\sigma_{Yp} & \text{for severe level} \end{cases} \quad (13)$$

Compressive residual stress at stiffener web:

$$\sigma_{rcx} = \begin{cases} -0.078\sigma_{Ys} & \text{for slight level} \\ -0.137\sigma_{Ys} & \text{for average level} \\ -0.195\sigma_{Ys} & \text{for severe level} \end{cases} \quad (14)$$

Width of the HAZ:

$$b'_p = b'_s = \begin{cases} 11.3 \text{ mm} & \text{for slight level} \\ 23.1 \text{ mm} & \text{for average level} \\ 29.9 \text{ mm} & \text{for severe level} \end{cases} \quad (15)$$

Collapse testing

Figure 9 shows the set-up of the physical collapse testing on the stiffened plate structures. The loaded edges are simply supported and the axial compressive loading is applied at the neutral axis of the panel cross section. A rigid circular bar at each side of loaded edges was inserted as shown in Fig.10 to reflect simply supported edge conditions along the loaded edges, i.e., by minimizing the rotational restraints.

Two types of unloaded edge condition are considered, namely free and simply support conditions, as shown in Figs.9(a) and 9(b) or 9(c), respectively. For the latter condition shown in Fig.9(b) or 9(c), a set of supporting jigs was attached to keep the unloaded edges straight. This condition was considered to reflect the behavior of stiffened panels in a continuous stiffened plate structure.

A total of 10 test structures with flat bar type stiffeners, namely ID40, 41, 42, 44, 45, 58, 59, 60, 62 and 63 were tested without the supporting jigs at unloaded edges, indicating a free edge condition. Figure 11 shows axial compressive loads versus shortening

curves of selected test structures. It is seen from Fig.11 that the structures exhibit nonlinear behavior until and after the ultimate strength is reached. This is partly due to initial imperfections.

- 1 bay SPM with initial deflection in CIP
- 1 bay SPM with initial deflection in CIS
- 2 bay SPM with initial deflection in CIP
- 2 bay SPM with initial deflection in CIS
- 1 bay PSC with initial deflection in CIP
- 1 bay PSC with initial deflection in CIS
- 2 bay PSC with initial deflection in CIP
- 2 bay PSC with initial deflection in CIS

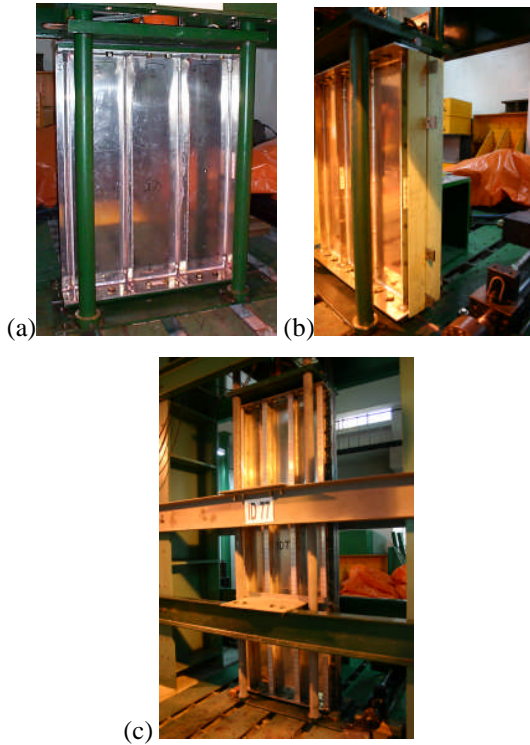


Fig.9: Test set-up for collapse testing on stiffened plate structures, (a) without supporting jigs at unloaded edges, (b), (c) with supporting jigs at unloaded edges to keep straight



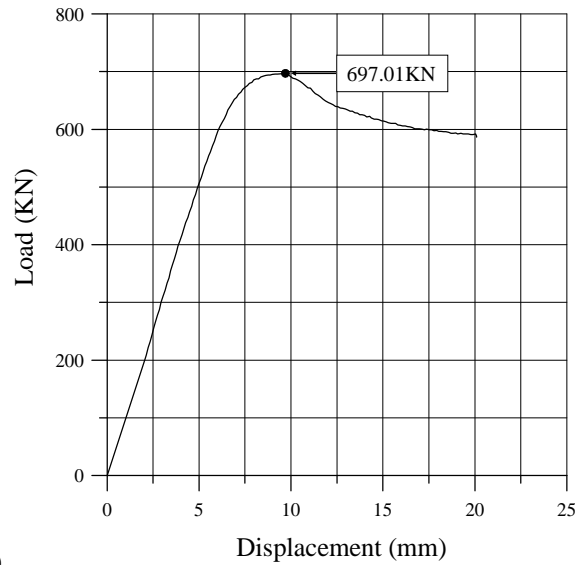
Fig.10: Simply supported condition at loaded edges and axial compressive loading at the neutral axis of the panel cross section

Nonlinear finite element analysis

Nonlinear finite element analysis (FEA) using ANSYS (2006) was carried out on the test structures by a comparison with FEA and test results. Since some arguments in terms of selecting relevant FEA modeling techniques still remain, 8 types of FEA modeling are in the present study considered with varying the extent of analysis and the direction of column type initial deflection of stiffeners (with the abbreviations of CIP = compression in plate side, CIS = compression in stiffener side, SPM = stiffened panel model, PSC = plate-stiffener combination model), namely

ID 1

Plate		Stiffener				
t	Material	h_w	t_w	b_f	t_f	Material
5 mm	5083-H116	55.7 mm	3.7 mm	40 mm	6.7 mm	5383-H112



ID 77

Plate		Stiffener				
t	Material	h_w	t_w	b_f	t_f	Material
8 mm	5083-H116	100 mm	6 mm	55 mm	8.2 mm	6082-T6

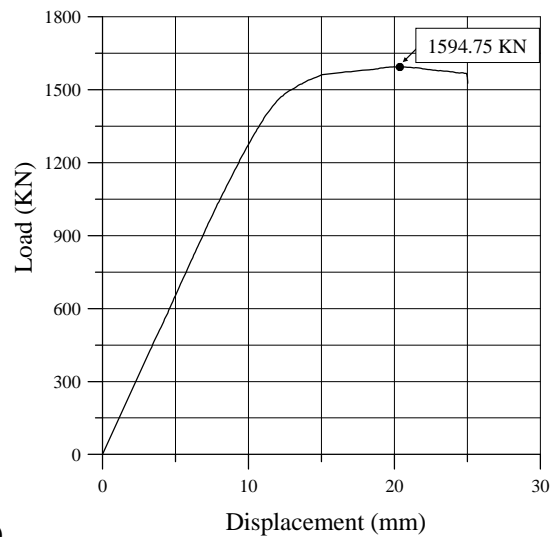


Fig.11: Axial compressive loads versus shortening curves for (a) ID1 and ID77, obtained by the experiment

In addition to the 8 types of modeling noted above, another 2 bay FE model was considered by reflecting the unloaded edges as being simply supported keeping them straight, namely

- 2 bay SPM with all (four) edges simply supported

While the test structures are primarily 1 bay system, i.e., considering the longitudinally stiffened panels between two transverse frames, 2 bay system including transverse frames as shown in Fig.12 are also considered in the present FEA to reflect the continuity support condition along the transverse frames in a continuous plate structure.

All of the 1 bay models are analyzed by a load control, while the 2 bay models are loaded by a displacement control, because of easier handling for the load application with regard to the neutral axis at the panel cross section.

After some convergence studies, the FE mesh size adopted has one plate-shell element representing the HAZ at plating and at the stiffener web. Ten plate-shell elements represent the plating between stiffeners and six elements model stiffener web, including the elements in the HAZ.

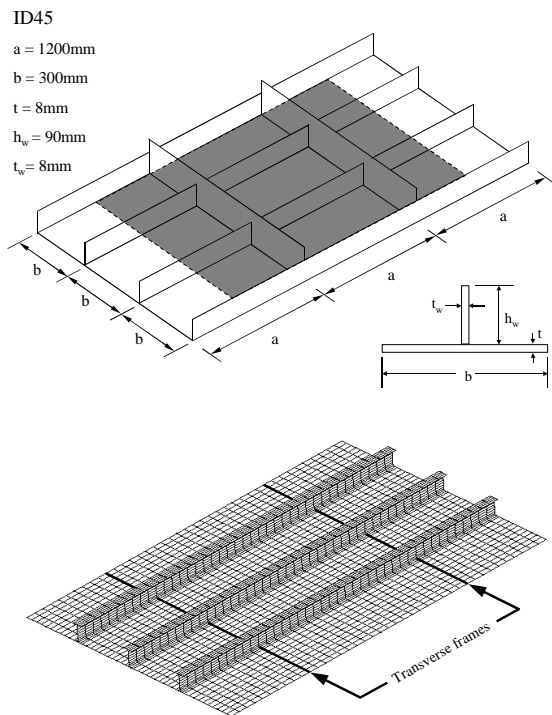


Fig.12(a): The extent and structural modeling for the 2 bay stiffened panel model (SPM) FEA

Figure 13 compares FEA solutions obtained by the 9 types of FE modeling noted above together with test data for two selected test panels until and after the ULS is reached. It is to be noted in Fig.13 that all FEA except for No. 10 were undertaken considering that the unloaded edges are free as in the actual testing, while No.10 was considered that the unloaded edges (as well as the loaded edges) are simply supported keeping them straight.

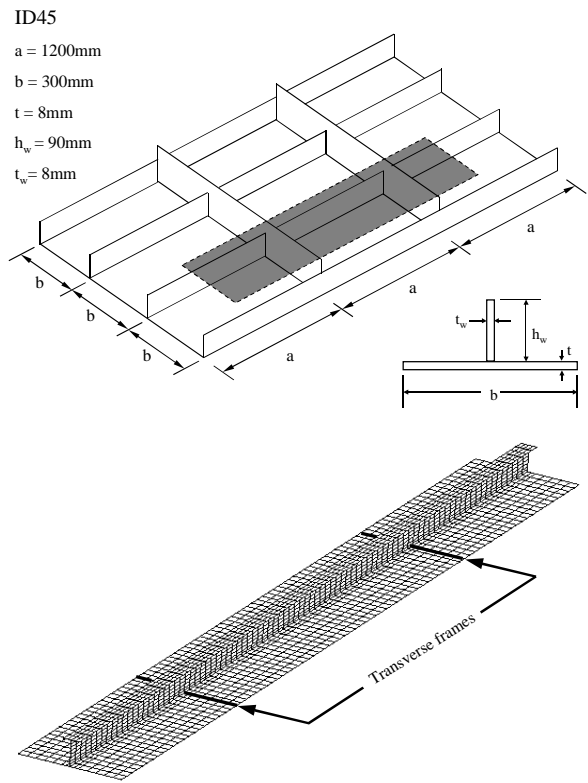


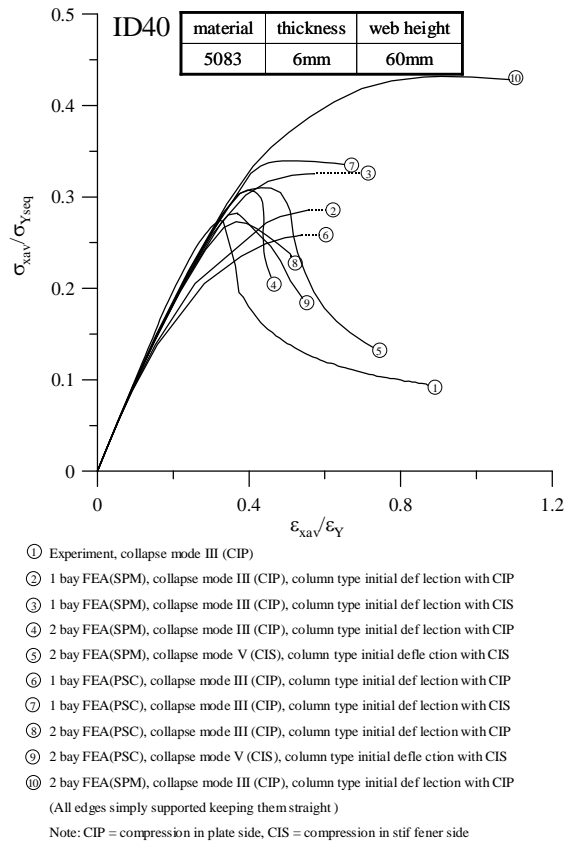
Fig.12(b): The extent and structural modeling for the 2 bay plate-stiffener combination (PSC) FEA

In the actual test, the panel ID 40 collapsed by column type collapse (Mode III) and ID 63 collapsed by stiffener tripping (Mode V). As would be expected, it is evident that the direction of column type initial deflection of stiffener significantly affects the FE solutions.

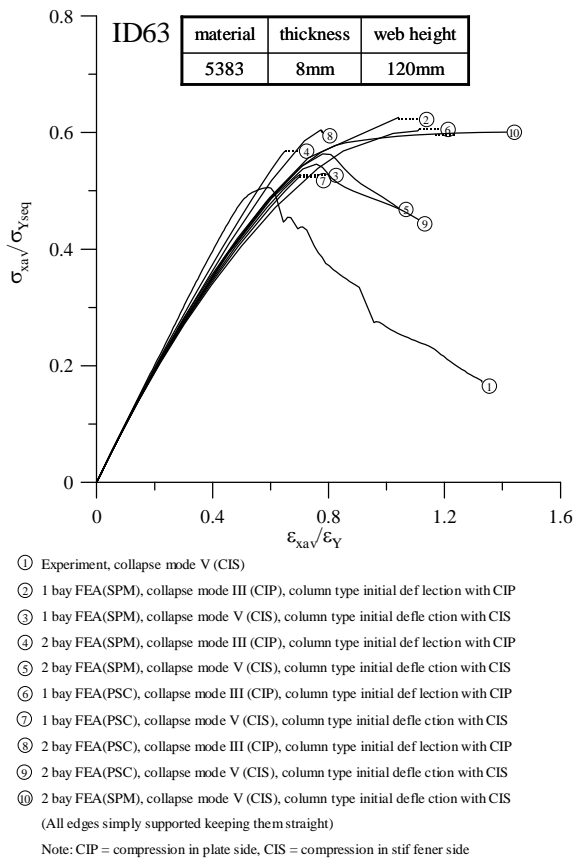
It is also seen that the 2 bay FEA always gives a larger ULS than 1 bay FEA. This is because the 2 bay FEA involves the rotational restraint effects along the transverse frames in the continuous plate structures.

It is to be noted that the different FE modeling approaches give quite different solutions. It is of vital importance to correctly reflect all of the influential parameters in the FE modeling in this regard. It is important to realize that the direction of column type initial deflections of stiffeners, among other factors may significantly affect the ultimate strength behavior when the magnitude of initial deflections is substantially large.

Also, it is evident that the model type or extent taken for the FE analysis must be determined carefully, while the real material stress-strain relationship rather than the elastic-perfectly plastic material approximation must always be employed unlike the ULS assessment of steel structures. Since softening in the HAZ plays a significant role on the welded aluminum plate structures, it must be carefully dealt with as well.



(a) 5083 panel



(b) 5383 panel

Fig.13: Comparison of FEA solutions as those obtained by 9 types of FE modeling together with test data for (a) a 5083 panel, (b) a 5383 panel

These aspects definitely make the aluminum panel ULS evaluation works cumbersome. In this regard, the present study adopts the following four types of FEA models for the test structures, namely

- 1 bay PSC model in CIP
- 1 bay PSC model in CIS
- 2 bay PSC model in CIP
- 2 bay PSC model in CIS

It is assumed that the material follows the elastic-perfectly plastic behavior neglecting strain-hardening effect. An ‘average level’ of initial imperfections including initial distortions, welding residual stresses and HAZ softening as measured for the test structures is applied for the FEA.

The mechanical properties (e.g., elastic modulus, yield stress) of aluminum alloys used for the present FEA were defined from the minimum values of classification society rules rather than actual values obtained from the tensile coupon tests.

Summary of experimental and numerical results

Table 3 summarizes the ultimate strengths of test structures together with collapse modes obtained by the experiment and nonlinear FEA. Theoretically, six primary modes of stiffened panel collapse under predominantly axial compressive loads are considered, namely (Paik & Thayamballi 2003)

- Mode I: Overall collapse of plating and stiffeners as a unit;
- Mode II: Collapse under predominantly biaxial compression;
- Mode III: Beam-column type collapse;
- Mode IV: Local buckling of stiffener web;
- Mode V: Tripping of stiffener;
- Mode VI: Gross yielding.

It was observed that the panel collapse patterns were clearly different depending on the panel geometries. For the ratio of stiffener web height to web thickness is relatively large, the stiffened panel mostly collapsed by lateral torsional buckling or tripping (Mode V), while the beam-column type collapse (Mode III) took place for panels with a smaller web height. For some panels with high T-bars, local web buckling (Mode IV) tends to occur.

Also, from the numerical computations, it is observed that the 2-bay FEA models give greater ultimate strength values than the 1-bay FEA models because the effect of rotational restraints along the transverse frames is taken into account in the 2-bay FEA models.

Closed-form ULS formulae

In ship design, the hull girder strength of ships is often governed by the buckling collapse behavior of deck or bottom panels. Hence the calculation of the buckling collapse strength of stiffened panels in deck and bottom structures under axial compressive loads, which are a primary load component due to ship's hull girder actions, is an essential task.

Closed-form empirical ULS formulae for aluminum stiffened plate structures under axial compressive loads are derived by the regression analysis of experimental and numerical database obtained from the present study (Paik 2007b).

To cover a wider range of plate slenderness ratio and column slenderness ratio in the developed ULS formulae, some additional FEA were undertaken for stiffened plate structures with different plate slenderness ratio and column slenderness ratio from those of prototype structures tested in the present study.

When the continuous stiffened plate structure is modeled as an assembly of plate-stiffener combinations, it is recognized that the ultimate compressive strength of the representative plate-stiffener combination is expressible as follows (Paik & Thayamballi 1997, 2003)

$$\frac{\sigma_u}{\sigma_{Yeq}} = [C_1 + C_2\lambda^2 + C_3\beta^2 + C_4\lambda^2\beta^2 + C_5\lambda^4]^{-0.5} \leq \frac{1}{\lambda^2} \quad (16)$$

where $C_1 \sim C_5 =$ coefficients to be determined from database.

For steel stiffened plate structures with an average level of weld induced initial imperfections, Paik and Thayamballi (1997, 2003) determined the coefficients of Eq.(16) by the least square method based on the experimental database as follows

$$\frac{\sigma_u}{\sigma_{Yeq}} = [0.995 + 0.936\lambda^2 + 0.170\beta^2 + 0.188\lambda^2\beta^2 - 0.067\lambda^4]^{-0.5} \leq \frac{1}{\lambda^2} \quad (17)$$

It is to be noted that σ_{Yeq}/λ^2 is the elastic buckling stress of a column member simply supported at both ends, and the ultimate strength of a column member should not be greater than the elastic buckling stress. Eq.(17) is useful for predicting the ultimate compressive strength of steel stiffened panels with Tee, angle or flat bars, the last type of stiffeners having relatively large column slenderness ratio, when an average level of initial imperfections is applied.

For aluminum stiffened plate structures, the use of a similar approach to steel stiffened plate structures was attempted but with different formulae for different types of stiffeners. We then suggest the following constants for aluminum stiffened plate structures with extruded or built-up T-bars when an average level of weld induced initial imperfections are applied, namely

$$\frac{\sigma_u}{\sigma_{Yeq}} = [1.318 + 2.759\lambda^2 + 0.185\beta^2 - 0.177\lambda^2\beta^2 + 1.003\lambda^4]^{-0.5} \leq \frac{1}{\lambda^2} \quad (18)$$

Figure 14 checks the accuracy of Eq.(18) together with Eq.(17) for steel stiffened plate structures. The bias and COV of Eq.(18) are 1.032 and 0.101, respectively. On the other hand, the ultimate strength of aluminum stiffened plate structures with flat bars can be given as a smaller value of the following two formula solutions, when an average level of initial imperfections is applied, namely

$$\frac{\sigma_u}{\sigma_{Yeq}} = \text{Min.} \left\{ \begin{aligned} & [2.500 - 0.588\lambda^2 + 0.084\beta^2 + 0.069\lambda^2\beta^2 + 1.217\lambda^4]^{-0.5} \leq \frac{1}{\lambda^2} \\ & [-16.297 + 18.776\lambda + 17.716\beta - 22.507\lambda\beta]^{-0.5} \end{aligned} \right. \quad (19)$$

Figure 15 checks the accuracy of Eq.(19) by a comparison with experimental and numerical results. Considering the uncertainty associated with initial imperfections and structural modeling techniques, among other factors, it is interesting to see the upper and lower limits of the panel ultimate strength with relevant deviations. Except for very thick panels with T-bars, i.e., with $\beta=2.08$ and 2.10, all experimental and numerical data of the panel ultimate strength are located in the range of $\pm 20\%$ deviations.

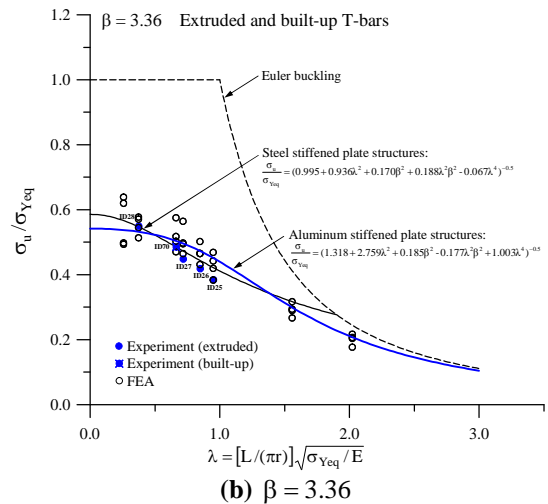
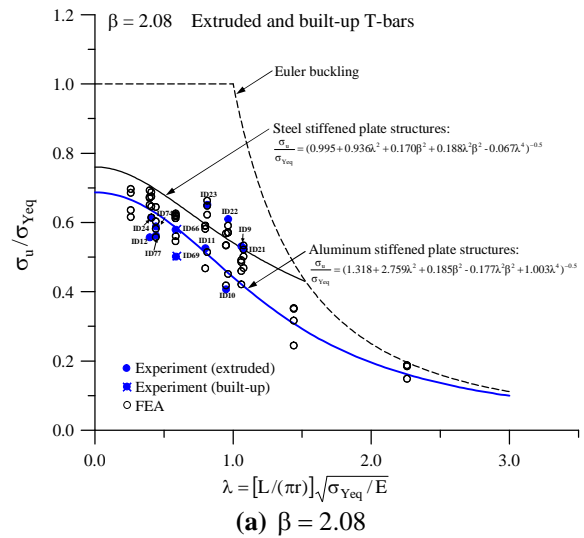


Fig.14: The accuracy of the closed-form empirical ULS formula, Eq.(18), for aluminum stiffened plate structures with T-bars, (a) $\beta = 2.08$, (b) $\beta = 3.36$

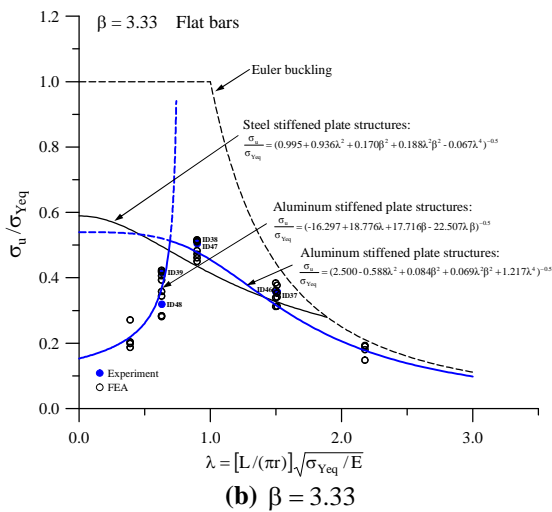
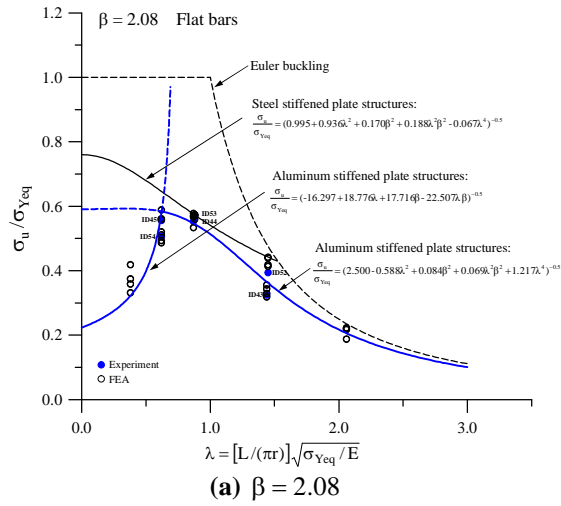


Fig.15 The accuracy of the closed-form empirical ULS formula, Eq.(19), for aluminum stiffened plate structures with flat bars, (a) $\beta = 2.08$, (b) $\beta = 3.33$

Concluding remarks

During the last decade, the application of aluminum alloys to marine structures such as high-speed vessels and littoral surface crafts has been rapidly increasing. To operate in increasingly harsher environments, the size of high-speed vessels has also grown. Subsequently, the structural design and building process to ensure the structural safety has become more complex in terms of limit state strength assessment and fabrication quality control among others.

In addition to more conventional structural design standards, the use of ULS design method will make possible to design and build very large aluminum high speed vessel structures that can operate in open ocean.

The aims of the present study have been to develop statistical database of fabrication related initial imperfections, and database of experimental and numerical results on the ultimate strength for aluminum stiffened plate structures, and also to derive closed-form empirical ULS formulae.

A total of 78 full-scale prototype aluminum structures, which are equivalent to sub-structures of an 80m long aluminum high speed vessel, were constructed

by MIG welding and a total of 6 types of fabrication related initial imperfections, which govern the load-carrying capacity were measured.

By statistical analyses of initial imperfection measurements, three different levels (i.e., slight, average and severe levels) of each of the six type initial imperfection parameters were determined which can be used as reference levels of initial imperfections in ultimate limit strength assessment in association with reliability analyses and code calibrations for welded aluminum marine structures.

Buckling collapse testing on the prototype structures was undertaken. The load-axial displacement curves were obtained until and after the ultimate strength is reached. Nonlinear elastic-plastic large deflection finite element analyses were performed for the prototype structures. The ultimate strength characteristics of the structures together with collapse modes were investigated in terms of plate slenderness ratio and column slenderness ratio as well as initial imperfections.

Closed-form empirical ULS formulas for aluminum stiffened plate structures were developed by the regression analysis of experimental and numerical ultimate strength database obtained from the present study.

It is believed and hoped that the database and insights developed from the present study will be very useful for ultimate limit state design and strength assessment of aluminum stiffened plate structures which are used for building very large high speed ships such as passenger ships, war ships, littoral surface or combat ships.

Acknowledgements

The present study was undertaken at the Ship and Offshore Structural Mechanics Laboratory (SSML), Pusan National University, Korea, which is a National Research Laboratory funded by the Korea Science and Engineering Foundation (Grant No. ROA-2006-000-10239-0). The authors are pleased to acknowledge the support of Ship Structure Committee, USA, Alcan Marine, France, and Hanjin Heavy Industries & Construction Company, Korea.

References

- Aalberg, A., Langseth, M. and Larsen, P.K. (2001). Stiffened aluminum panels subjected to axial compression. *Thin-Walled Structures*, Vol.39, pp.861-885.
- Antoniou, A.C. (1980). On the maximum deflection of plating in newly built ships. *Journal of Ship Research*, Vol.24, No.1, pp.31-39
- Antoniou, A.C., Lavidas, M. and Karvounis, G. (1984). On the shape of post-welding deformations of plate panels in newly built ships. *Journal of Ship Research*, Vol.28, No.1, pp.1-10
- Bradfield, C.D. (1974). Analysis of measured distortions in steel box-girder bridges. Cambridge University Engineering Department, Report CUED/C-Struct/TR42.

- Carlsen, C.A. and Czujko, J. (1978). The specification of postwelding distortion tolerances for stiffened plates in compression. *The Structural Engineer*, Vol.56A, No.5, pp.133-141
- Czujko, J. and Kmiecik, M. (1975). Post welding distortions of ship shell plating. Ship Research Institute Report No.4-5, Technical University of Szczecin, Poland.
- Czujko, J. (1980). Probabilistic estimation of load carrying capacity of axially compressed plates with random post-welding distortions. The Norwegian Institute of Technology, The University of Trondheim, Norway.
- DNV (2003). Rules for ships / high speed, light craft and naval surface craft. Det Norske Veritas, Oslo, Norway
- Ellis, L.G. (1977). A statistical appraisal of the measured deformations in several steel box girder bridge. *Journal of Strain Analysis*, Vol.12, No.2, pp.97-106.
- EN 13195-1 (2002). Aluminum and aluminum alloys: wrought and cast products for marine applications (shipbuilding, marine and offshore). European Standard: French Standard, Association Francaise de Normalisation (AFNOR), Paris.
- Faulkner, D. (1975). A review of effective plating for use in the analysis of stiffened plating in bending and compression. *Journal of Ship Research*, Vol.19, No.1, pp.1-17
- Hopperstad, O.S., Langseth, M. and Hanssen, L. (1998). Ultimate compressive strength of plate elements in aluminum: Correlation of finite element analyses and tests. *Thin-Walled Structures*, Vol. 29, pp.31-46.
- Hopperstad, O.S., Langseth, M. and Tryland, T. (1999). Ultimate strength of aluminum alloy outstands in compression: experiments and simplified analyses. *Thin-Walled Structures*, Vol. 34, pp. 279-294.
- Kmiecik, M (1970). The load carrying capacity of axially loaded longitudinally stiffened plates having initial deformation. Ship Research Institute Report No.R80, Technical University of Szczecin, Poland.
- Kmiecik, M. (1971). Behavior of axially loaded simply supported long rectangular plates having initial deformations. SFI, Trondheim, Norway.
- Kmiecik, M. (1981). Factors affecting the load-carrying capacity of plates. Ship Research Institute Report No.115, Technical University of Szczecin, Poland.
- Kmiecik, M. (1986-1987). A review of fabrication distortion tolerances for ship plating in the light of the compressive strength of plates. Paper No.6, Lloyd's Register Technical Association, London.
- Kmiecik, M., Jastrzebski, T. and Kuzniar, J. (1995). Statistics of ship plating distortions. *Marine Structures*, Vol.8, pp.119-132.
- Kontoleon, M.J., Preftitsi, F.G. and Baniotopoulos, C.C. (2000). Butt-welded aluminum joints: a numerical study of the HAZ effect on the ultimate tension strength. The paramount role of joints into the reliable response of structures, Edited by C.C. Baniotopoulos and F. Wald, pp. 337-346.
- Masubuchi, K. (1980). Analysis of welded structures – Residual stresses, distortion and their consequences. Pergamon Press, Oxford.
- Matsuoka, K., Tanaka, Y. and Fujita, Y. (1998). Buckling strength of lightened aluminum hull structures. Proceedings of INALCO'98, International Conference on Aluminum Structural Design, Cambridge, UK, April 15-17.
- Mazzolani, F.M. (1985). Aluminum alloy structures. Pitman Advanced Publishing Program, Boston.
- Mofflin, D.S. (1983). Plate buckling in steel and aluminum. Ph.D. Thesis, University of Cambridge, UK.
- Mofflin, D.S. and Dwight, J.B. (1984). Buckling of aluminum plates in compression. In: *Behavior of Thin-Walled Structures*, Elsevier, pp.399-427.
- Paik, J.K., et al. (2006). The statistics of weld induced initial imperfections in aluminum stiffened plate structures for marine application. *International Journal of Maritime Engineering*, Vol.148, Part A4, pp.1-50.
- Paik, J.K. (2007a). Characteristics of welding induced initial deflections in welded aluminum plates. *Thin-Walled Structures*, Vol.45, pp.493-501.
- Paik, J.K. (2007b). Empirical formulations for predicting the ultimate compressive strength of welded aluminum stiffened panels. *Thin-Walled Structures*, Vol.45, pp.171-184.
- Paik, J.K. and Thayamballi, A.K. (1997). An empirical formulation for predicting the ultimate compressive strength of stiffened panels. Proceedings of International Offshore and Polar Engineering Conference, Honolulu, Vol.IV, pp.328-338.
- Paik, J.K. and Thayamballi, A.K. (2003). Ultimate limit state design of steel-plated structures. John Wiley & Sons, Chichester, UK.
- Paik, J.K. and Thayamballi, A.K. (2007). Ship-shaped offshore installations: Design, building, and operation. Cambridge University Press, Cambridge, UK.
- Paik, J.K., Thayamballi, A.K. and Lee, J.M. (2004). Effect of initial deflection shape on the ultimate strength behavior of welded steel plates under biaxial compressive loads. *Journal of Ship Research*, Vol.48, No.1, pp.45-60.
- Paik, J.K. and Duran, A. (2004). Ultimate strength of aluminum plates and stiffened panels for marine applications. *Marine Technology*, Vol. 41, No 3, pp. 108-121.
- Paik, J.K., Hughes, O.F., Hess, P.E. and Renaud, C. (2005). Ultimate limit state design technology for aluminum multi-hull ship structures. *SNAME Transactions*, Vol. 113, pp.270-305.
- Raynaud, G.M. (1995). New aluminum products for high speed light crafts. Building High-speed Aluminum Marine Vessels in Victoria – A Feasibility Study, Business Victoria, Melbourne, Australia.
- Smith, C.S. and Dow, R.S. (1984). Effects of localized imperfections on compressive strength of long rectangular plates. *Journal of Constructional Steel Research*, Vol.4, pp.51-76

- Smith, C.S., Davidson, P.C., Chapman, J.C. and Dowling, P.J. (1988). Strength and stiffness of ships' plating under in-plane compression and tension, RINA Transactions, Vol. 130, pp. 277-296.
- Somerville, W.L., Swan, J.W. and Clarke, J.D. (1977). Measurement of residual stresses and distortions in stiffened panels. Journal of Strain Analysis, Vol.12, No.2, pp.107-116.
- Timoshenko, S.P. and Gere, J.M. (1961). Theory of elastic stability. McGraw-Hill, New York.
- Timoshenko, S.P. and Woinowsky-Krieger, S. (1981). Theory of plates and shells. McGraw-Hill, New York.
- Tanaka, Y. and Matsuoka, K. (1997). Buckling strength of lightened aluminum hull structures. Proceedings of the 7th International Offshore and Polar Engineering Conference, Vol.4, Honolulu, pp.790-797.
- Ueda, Y. and Yao, T. (1985). The influence of complex initial deflection modes on the behavior and ultimate strength of rectangular plates in compression. Journal of Constructional Steel Research, Vol.5, pp.265-302
- Zha, Y., Moan, T. and Hanken, E. (2000). Experimental and numerical studies of torsional buckling of stiffener in aluminum panels. Proceedings of the 8th International Offshore and Polar Engineering Conference, Seattle, pp.249-255.
- Zha, Y. and Moan, T. (2001). Ultimate strength of stiffened aluminum panels with predominantly torsional failure modes. Thin-Walled Structures, Vol.39, No.8, pp.631-648.
- Zha, Y. and Moan, T. (2003). Experimental and numerical collapse prediction of flat bar stiffeners in aluminum panels. Journal of Structural Engineering, Vol.129, No.2, pp.160-168.

Table 1: Overall characteristics of the 78 prototype structures

One bay test plate structures (1200 mm × 1000 mm) with no replications:

ID	Plate		Stiffener					
	t(mm)	Alloy and temper	Type	h _w (mm)	t _w (mm)	b _f (mm)	t _f (mm)	Alloy and temper
1	5	5083-H116	Extruded Tee	55.7	3.7	40	(6.7)	5383-H112
2	5	5083-H116	Extruded Tee	66.1	4	40	(5.7)	5383-H112
3	5	5083-H116	Extruded Tee	76.8	4	45	(5.6)	5383-H112
4	5	5083-H116	Extruded Tee	135	6	55	(8.2)	5383-H112
5	6	5083-H116	Extruded Tee	55.7	3.7	40	(6.7)	5383-H112
6	6	5083-H116	Extruded Tee	66.1	4	40	(5.7)	5383-H112
7	6	5083-H116	Extruded Tee	76.8	4	45	(5.6)	5383-H112
8	6	5083-H116	Extruded Tee	135	6	55	(8.2)	5383-H112
9	8	5083-H116	Extruded Tee	55.7	3.7	40	(6.7)	5383-H112
10	8	5083-H116	Extruded Tee	66.1	4	40	(5.7)	5383-H112
11	8	5083-H116	Extruded Tee	76.8	4	45	(5.6)	5383-H112
12	8	5083-H116	Extruded Tee	135	6	55	(8.2)	5383-H112
13	5	5083-H116	Extruded Tee	55.7	3.7	40	(6.7)	6082-T6
14	5	5083-H116	Extruded Tee	66.1	4	40	(5.7)	6082-T6
15	5	5083-H116	Extruded Tee	76.8	4	45	(5.6)	6082-T6
16	5	5083-H116	Extruded Tee	135	6	55	(8.2)	6082-T6
17	6	5083-H116	Extruded Tee	55.7	3.7	40	(6.7)	6082-T6
18	6	5083-H116	Extruded Tee	66.1	4	40	(5.7)	6082-T6
19	6	5083-H116	Extruded Tee	76.8	4	45	(5.6)	6082-T6
20	6	5083-H116	Extruded Tee	135	6	55	(8.2)	6082-T6
21	8	5083-H116	Extruded Tee	55.7	3.7	40	(6.7)	6082-T6
22	8	5083-H116	Extruded Tee	66.1	4	40	(5.7)	6082-T6
23	8	5083-H116	Extruded Tee	76.8	4	45	(5.6)	6082-T6
24	8	5083-H116	Extruded Tee	135	6	55	(8.2)	6082-T6
25	5	5383-H116	Extruded Tee	55.7	3.7	40	(6.7)	5383-H112

Table 1: Overall characteristics of the 78 prototype structures (continued)

ID	Plate		Stiffener					
	t(mm)	Alloy and temper	Type	h _w (mm)	t _w (mm)	b _f (mm)	t _f (mm)	Alloy and temper
26	5	5383-H116	Extruded Tee	66.1	4	40	(5.7)	5383-H112
27	5	5383-H116	Extruded Tee	76.8	4	45	(5.6)	5383-H112
28	5	5383-H116	Extruded Tee	135	6	55	(8.2)	5383-H112
29	6	5383-H116	Extruded Tee	55.7	3.7	40	(6.7)	5383-H112
30	6	5383-H116	Extruded Tee	66.1	4	40	(5.7)	5383-H112
31	6	5383-H116	Extruded Tee	76.8	4	45	(5.6)	5383-H112
32	6	5383-H116	Extruded Tee	135	6	55	(8.2)	5383-H112
33	8	5383-H116	Extruded Tee	55.7	3.7	40	(6.7)	5383-H112
34	8	5383-H116	Extruded Tee	66.1	4	40	(5.7)	5383-H112
35	8	5383-H116	Extruded Tee	76.8	4	45	(5.6)	5383-H112
36	8	5383-H116	Extruded Tee	135	6	55	(8.2)	5383-H112
37	5	5083-H116	Flat	60	5	-	-	5083-H116
38	5	5083-H116	Flat	90	5	-	-	5083-H116
39	5	5083-H116	Flat	120	5	-	-	5083-H116
40	6	5083-H116	Flat	60	6	-	-	5083-H116
41	6	5083-H116	Flat	90	6	-	-	5083-H116
42	6	5083-H116	Flat	120	6	-	-	5083-H116
43	8	5083-H116	Flat	60	8	-	-	5083-H116
44	8	5083-H116	Flat	90	8	-	-	5083-H116
45	8	5083-H116	Flat	120	8	-	-	5083-H116
46	5	5083-H116	Flat	60	5	-	-	5383-H116
47	5	5083-H116	Flat	90	5	-	-	5383-H116
48	5	5083-H116	Flat	120	5	-	-	5383-H116
49	6	5083-H116	Flat	60	6	-	-	5383-H116
50	6	5083-H116	Flat	90	6	-	-	5383-H116
51	6	5083-H116	Flat	120	6	-	-	5383-H116
52	8	5083-H116	Flat	60	8	-	-	5383-H116
53	8	5083-H116	Flat	90	8	-	-	5383-H116
54	8	5083-H116	Flat	120	8	-	-	5383-H116
55	5	5383-H116	Flat	60	5	-	-	5383-H116
56	5	5383-H116	Flat	90	5	-	-	5383-H116
57	5	5383-H116	Flat	120	5	-	-	5383-H116
58	6	5383-H116	Flat	60	6	-	-	5383-H116
59	6	5383-H116	Flat	90	6	-	-	5383-H116
60	6	5383-H116	Flat	120	6	-	-	5383-H116
61	8	5383-H116	Flat	60	8	-	-	5383-H116
62	8	5383-H116	Flat	90	8	-	-	5383-H116
63	8	5383-H116	Flat	120	8	-	-	5383-H116

Table 1: Overall characteristics of the 78 prototype structures (continued)

ID	Plate		Stiffener					
	t(mm)	Alloy and temper	Type	h_w (mm)	t_w (mm)	b_f (mm)	t_f (mm)	Alloy and temper
64	5	5083-H116	Built-up Tee	80	5	60	5	5083-H116
65	6	5083-H116	Built-up Tee	60	5	60	5	5083-H116
66	8	5083-H116	Built-up Tee	100	5	60	5	5083-H116
67	5	5083-H116	Built-up Tee	80	5	60	5	5383-H116
68	6	5083-H116	Built-up Tee	60	5	60	5	5383-H116
69	8	5083-H116	Built-up Tee	100	5	60	5	5383-H116
70	5	5383-H116	Built-up Tee	80	5	60	5	5383-H116
71	6	5383-H116	Built-up Tee	60	5	60	5	5383-H116
72	8	5383-H116	Built-up Tee	100	5	60	5	5383-H116

One bay test plate structures (1000 mm × 1000 mm):

ID	Plate		Stiffener					
	t(mm)	Alloy and temper	Type	h_w (mm)	t_w (mm)	b_f (mm)	t_f (mm)	Alloy and temper
73	6	5083-H116	Extruded Tee	76.8	4	45	(5.6)	6082-T6
74	8	5083-H116	Extruded Tee	100	6	55	(8.2)	6082-T6
75	8	5383-H116	Extruded Tee	100	6	55	(8.2)	5383-H112

Three bay test plate structures (3000 mm × 1000 mm):

ID	Plate		Stiffener					
	t(mm)	Alloy and temper	Type	h_w (mm)	t_w (mm)	b_f (mm)	t_f (mm)	Alloy and temper
76	6	5083-H116	Extruded Tee	76.8	4	45	(5.6)	6082-T6
77	8	5083-H116	Extruded Tee	100	6	55	(8.2)	6082-T6
78	8	5383-H116	Extruded Tee	100	6	55	(8.2)	5383-H112

Notes: t = plate thickness, h_w = web height (excluding flange thickness), t_w = web thickness, b_f = flange width, t_f = flange thickness, t_f where given in brackets indicates the effective value of for an idealized plate-stiffener combination with the same moment of inertia as the actual case.

Table 2: Minimum values of mechanical properties of aluminum alloys used for the construction of prototype structures (DNV 2003)

Alloy and temper	Yield strength of base metal (N/mm ²)	Tensile strength of base metal (N/mm ²)	Elongation of base metal (%)	Type of production	Yield strength of welded material (N/mm ²)
5083-H116	215	305	10	Rolled	125
5383-H116	220	305	10	Rolled	145
5383-H112	190	310	13	Extruded	145
6082-T6	240	290	5	Extruded	100

Note: Elastic modulus $E = 70,000 \text{ N/mm}^2$, Poisson's ratio $\nu = 0.33$.

Table 3: Summary of the ultimate strengths of test structures together with collapse modes obtained by FEA and experiment

ID	Exp.		FEA							
			1 bay-CIP		1 bay-CIS		2 bay-CIS		2 bay-CIS	
	σ_u/σ_{Yeq}	Mode	σ_u/σ_{Yeq}	Mode	σ_u/σ_{Yeq}	Mode	σ_u/σ_{Yeq}	Mode	σ_u/σ_{Yeq}	Mode
ID1	0.462	III	0.380	III	0.413	III	0.474	III	0.449	V
ID2	0.487	V	0.426	III	0.459	III	0.508	III	0.471	V
ID3	0.517	III,IV	0.460	III	0.490	III	0.517	III	0.492	V
ID4	0.546	IV,V	0.452	III	0.456	III	0.550	V	0.562	V
ID5	0.448	III	0.434	III	0.482	III	0.478	III	0.471	V
ID6	0.530	III	0.490	III	0.536	III	0.516	III	0.495	V
ID7	0.516	III	0.521	III	0.559	III	0.554	III	0.526	V
ID8	0.615	V	0.554	III	0.560	III	0.604	V	0.590	V
ID9	0.531	V	0.459	III	0.421	V	0.485	III	0.491	V
ID10	0.407	V	0.568	V	0.417	V	0.533	III	0.534	V
ID11	0.526	V	0.589	V	0.467	V	0.590	III	0.581	V
ID12	0.557	V	0.673	III	0.692	III	0.670	V	0.650	V
ID13	0.435	III	0.354	III	0.390	III	0.491	III	0.474	V
ID14	0.477	III	0.399	III	0.434	III	0.531	III	0.479	V
ID15	0.492	III,IV	0.433	III	0.464	III	0.602	III	0.543	V
ID16	0.596	III,IV	0.505	III	0.511	III	0.582	V	0.593	V
ID17	0.431	III	0.402	III	0.452	III	0.506	III	0.491	V
ID18	0.460	III	0.458	III	0.528	III	0.532	III	0.500	V
ID19	0.513	III,IV	0.487	III	0.529	III	0.602	III	0.556	V
ID20	0.627	III,IV	0.503	III	0.514	III	0.575	V	0.582	V
ID21	0.525	III	0.501	III	0.468	V	0.521	III	0.533	V
ID22	0.610	V	0.590	III	0.451	V	0.570	III	0.570	V
ID23	0.651	IV,V	0.622	III	0.514	V	0.662	III	0.647	V
ID24	0.613	III,IV	0.614	III	0.645	III	0.674	V	0.687	V
ID25	0.384	III	0.383	III	0.419	III	0.468	III	0.442	V
ID26	0.418	III	0.430	III	0.464	III	0.501	III	0.464	V
ID27	0.448	III,IV	0.464	III	0.494	III	0.564	III	0.497	V
ID28	0.549	III,IV	0.513	III	0.544	III	0.577	V	0.570	V
ID29	0.447	V	0.433	III	0.485	III	0.486	III	0.475	V
ID30	0.515	V	0.488	III	0.537	III	0.532	III	0.508	V
ID31	0.494	III,IV	0.525	III	0.564	III	0.564	III	0.543	V
ID32	0.548	III,IV	0.552	III	0.590	III	0.608	V	0.594	V
ID33	0.544	V	0.518	III	0.407	V	0.551	III	0.538	V
ID34	0.538	V	0.536	III	0.401	V	0.575	III	0.564	V
ID35	0.491	V	0.564	V	0.448	V	0.612	III	0.600	V

ID	Exp.		FEA							
	σ_u/σ_{Yeq}	Mode								
ID36	0.516	V	0.602	III	0.628	III	0.664	V	0.645	V
ID37	0.356	III	0.312	III	0.339	III	0.361	III	0.384	V
ID38	0.512	III	0.471	III	0.460	V	0.513	III	0.510	V
ID39	0.416	V	0.406	III	0.393	V	0.423	III	0.418	V
ID40	0.301	III	0.290	III	0.304	III	0.312	III	0.326	V
ID41	0.463	III	0.457	III	0.465	III	0.523	III	0.482	V
ID42	0.430	V	0.427	III	0.413	V	0.465	III	0.440	V

Table 3: Summary of the ultimate strengths of test structures together with collapse modes obtained by FEA and experiment (continued)

ID	Exp.		FEA							
	σ_u/σ_{Yeq}	Mode	1 bay-CIP		1 bay-CIS		2 bay-CIS		2 bay-CIS	
			σ_u/σ_{Yeq}	Mode	σ_u/σ_{Yeq}	Mode	σ_u/σ_{Yeq}	Mode	σ_u/σ_{Yeq}	Mode
ID43	0.325	V	0.318	III	0.329	V	0.343	III	0.355	V
ID44	0.553	V	0.543	III	0.570	III	0.577	III	0.566	V
ID45	0.556	V	0.520	III	0.560	V	0.588	III	0.558	V
ID46	0.357	III	0.313	III	0.341	III	0.353	III	0.377	V
ID47	0.504	V	0.472	III	0.483	V	0.514	III	0.516	V
ID48	0.319	V	0.284	III	0.281	V	0.344	III	0.358	V
ID49	0.271	III	0.264	III	0.288	III	0.314	III	0.327	V
ID50	0.559	V	0.522	III	0.545	V	0.567	III	0.569	V
ID51	0.513	V	0.507	III	0.484	V	0.530	III	0.495	V
ID52	0.394	III	0.413	III	0.418	V	0.451	III	0.449	V
ID53	0.572	III	0.572	III	0.559	III	0.581	III	0.583	V
ID54	0.506	V	0.493	III	0.486	V	0.560	III	0.511	V
ID55	0.323	III	0.295	III	0.315	III	0.332	III	0.343	V
ID56	0.467	V	0.440	III	0.411	V	0.476	III	0.450	V
ID57	0.386	V	0.369	III	0.349	V	0.425	III	0.410	V
ID58	0.312	III	0.292	III	0.306	III	0.312	III	0.324	V
ID59	0.432	III	0.436	III	0.446	III	0.472	III	0.447	V
ID60	0.419	V	0.435	III	0.389	V	0.402	III	0.422	V
ID61	0.405	III	0.385	III	0.380	V	0.397	III	0.405	V
ID62	0.687	V	0.575	III	0.635	III	0.616	III	0.621	V
ID63	0.561	V	0.570	III	0.556	V	0.579	III	0.558	V
ID64	0.518	III,IV	0.465	III	0.500	III	0.567	III	0.522	V
ID65	0.508	III	0.468	III	0.500	III	0.510	III	0.486	V
ID66	0.579	V	0.612	III	0.545	V	0.612	III	0.619	V
ID67	0.526	III,IV	0.464	III	0.520	III	0.579	III	0.523	V
ID68	0.466	III,IV	0.467	III	0.523	III	0.510	III	0.487	V
ID69	0.501	V	0.617	III	0.560	V	0.625	III	0.621	V

			FEA							
ID70	0.485	III,IV	0.469	III	0.502	III	0.574	III	0.517	V
ID71	0.460	III	0.472	III	0.531	III	0.505	III	0.480	V
ID72	0.619	V	0.633	III	0.547	V	0.619	III	0.614	V
ID73	0.526	III	0.520	III	0.554	III	-	-	-	-
ID74	0.589	III,IV	0.603	III	0.644	III	-	-	-	-
ID75	0.592	III,IV	0.612	III	0.651	III	-	-	-	-
ID76	0.529	III	-	-	-	-	0.564	III	0.541	V
ID77	0.563	III,IV	-	-	-	-	0.581	III	0.557	V
ID78	0.607	III	-	-	-	-	0.643	III	0.620	V